THE ARM PROGRAM'S WATER VAPOR INTENSIVE OBSERVATION PERIODS

Overview, Initial Accomplishments, and Future Challenges

BY H. E. REVERCOMB, D. D. TURNER,* D. C. TOBIN, R. O. KNUTESON, W. F. FELTZ, J. BARNARD, J. BÖSENBERG, S. CLOUGH, D. COOK, R. FERRARE, J. GOLDSMITH, S. GUTMAN, R. HALTHORE, B. LESHT, J. LILJEGREN, H. LINNÉ, J. MICHALSKY, V. MORRIS, W. PORCH, S. RICHARDSON, B. SCHMID, M. SPLITT, T. VAN HOVE, E. WESTWATER, AND D. WHITEMAN

Results from a series of experiments focused on the lower troposphere have pointed the way to significantly improving the accuracy of water vapor measurements.

Water vapor is the dominant greenhouse gas in the atmosphere. It also plays an important role in the life cycle of clouds and precipitation, the transfer of latent and sensible heat, and in atmospheric chemistry. Unlike long-lived trace gases (e.g., CO_2, N_2O, CH_4), water vapor varies by several orders of magnitude with height, and can change by a factor of 2 or more in a very short period of time at any given location or over a short vertical distance (tens of meters). Since 1995, the U.S. Department of Energy's Atmospheric Radiation Measurement (ARM) (see appendix A for a list of acronyms and

AFFILIATIONS: REVERCOMB, TOBIN, KNUTESON, FELTZ—University of Wisconsin—Madison, Madison, Wisconsin; TURNER, BARNARD, MORRIS—Pacific Northwest National Laboratory, Richland, Washington; BÖSENBERG, LINNÉ—Max Planck Institute for Meteorology, Hamburg, Germany; CLOUGH—Atmospheric and Environmental Research, Inc., Lexington, Massachusetts; COOK, LESHT, LILJEGREN—Argonne National Laboratory, Argonne, Illinois; FERRARE—NASA Langley Research Center, Hampton, Virginia; GOLDSMITH—Sandia National Laboratories, Livermore, California; GUTMAN—NOAA/Forecast Systems Laboratory, Boulder, Colorado; HALTHORE—Naval Research Laboratory, Monterey, California; MICHALSKY—University at Albany, State University of New York, Albany, New York; PORCH—Los Alamos National Laboratory, Los Alamos, New Mexico; RICHARDSON—Cooperative Institute for Mesoscale Meteorological Studies, and University of Oklahoma, Norman Oklahoma; SCHMID—NASA Ames Research Center, Moffett Field, California; SPLITT—University of Utah, Salt Lake City, Utah; VAN HOVE—University Cooperation for Atmospheric Research, Boulder, Colorado; WESTWATER—Cooperative Institute for Research in Environmental Sciences, Boulder, Colorado; WHITEMAN—NASA Goddard Space Flight Center, Greenbelt, Maryland
*On leave from Climate Dynamics Group, Pacific Northwest National Laboratory, Richland, Washington
CORRESPONDING AUTHOR: David D. Turner, University of Wisconsin—Madison, 1225 W. Dayton St., Madison, WI 53706
E-mail: dturner@ssec.wisc.edu
DOI: 10.1175/BAMS-84-2-217

In final form 8 July 2002

their expansions) program has placed special emphasis on characterizing the current water vapor measurement capabilities and on developing improvements in measuring water vapor in the atmosphere. This paper summarizes some of the considerable progress made to date in measuring atmospheric water vapor.

The ARM program (information available online at www.arm.gov) was designed to collect a long-term (> 10 yr) dataset consisting of atmospheric state, radiative fluxes, and surface properties to (U.S. Department of Energy 1996) 1) relate observed radiative fluxes and radiances in the atmosphere to the temperature and composition of the atmosphere, specifically water vapor and clouds, and to surface properties; and 2) develop and test parameterizations that can be used to accurately predict radiative properties and to model the radiative interactions involving water vapor and clouds in the atmosphere.

To accomplish these objectives, ARM has developed three Cloud and Radiation Testbed (CART) sites, which are located in the southern Great Plains (SGP), the North Slope of Alaska (NSA), and in the tropical western Pacific (TWP) (Stokes and Schwartz 1994). These sites have numerous in situ sensors, and active and passive remote sensors. The SGP site, which is the most comprehensively equipped site, consists of a network of observing sites covering a domain similar in size to a grid cell of a general circulation or single-column model (roughly 250 km by 300 km). The CART sites are important for validating various satellite-derived products, allowing these high quality observations to be "transferred" globally.

A series of water vapor intensive observation periods (WVIOPs) have been organized and conducted at the Central Facility of the SGP site (Fig. 1). The first goal of these IOPs is to characterize the accuracy of the current water vapor measurements, especially the operational observations made by the ARM program. The second goal is to improve the accuracy of these observations by combining them to obtain the best possible water vapor measurements under a wide range of conditions (e.g., dry–moist, clear–cloudy, day–night, etc.). These WVIOPs are summarized in Table 1. The first four IOPs focused on measuring water vapor in the lower troposphere, which dominates the longwave surface radiation budget. The fifth IOP, the ARM–First International Satellite Cloud Climatology Project (ISCCP) Regional Experiment (FIRE) Water Vapor Experiment (AFWEX), was conducted in conjunction with the National Aeronautics and Space Administration (NASA's) FIRE program and focused on the water vapor in the middle and upper troposphere, which dominates the emission of radiation to space. While the two altitude regimes overlap considerably, this paper concentrates on the first three IOPs focusing on the lower-tropospheric water vapor.

MOTIVATION AND HYPOTHESES. During the mid-1980s, an international program, the Inter-

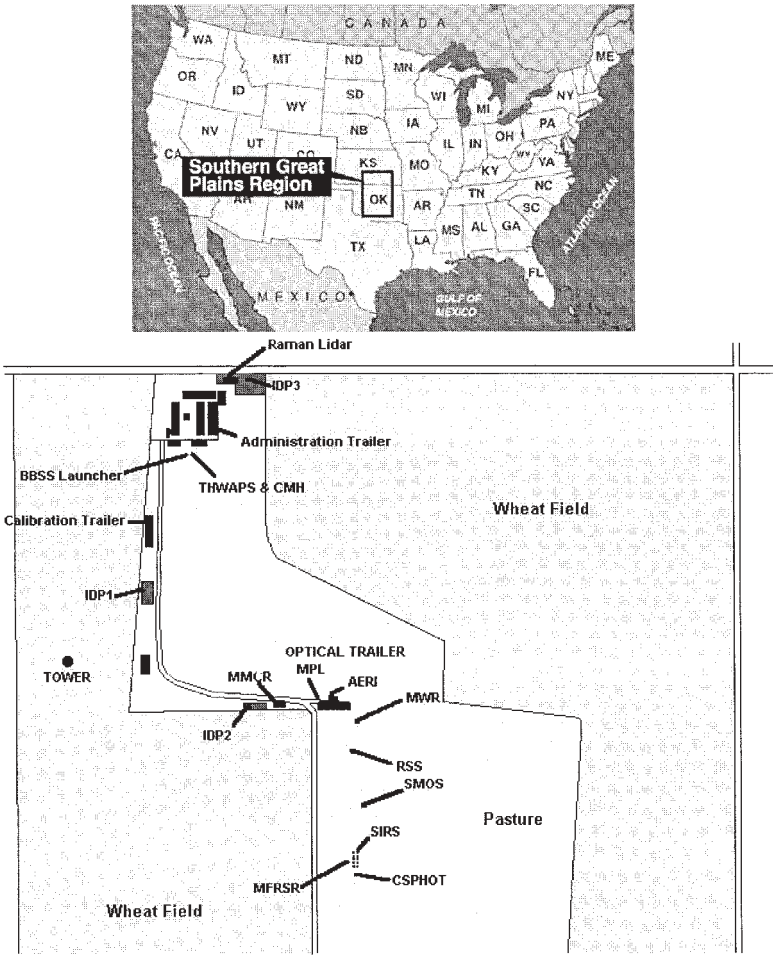

Fig. 1. Location of the ARM southern Great Plains CART site. The Central Facility is located in the center of this domain near Lamont, OK, and is approximately 0.25 mi on a side. The location of the various ARM operational water vapor instruments at the Central Facility, as well as locations of the Instrument Development Program pads where the guest instruments were located, are shown.

Table 1. WVIOP dates and primary results.

IOP name	IOP dates	Comments
1996 WVIOP	10–30 Sep 1996	Primary results: large (> 25%) sonde-to-sonde differences characterized and found to act to first order as a height-independent scale factor; stable MWR observations used to scale radiosonde moisture profiles, which is shown to significantly reduce sonde variability; in situ Qualimetrics sensors on instrumented tower are found to be inadequate and are replaced; demonstrated differences less than 5% between the two Raman lidars for all altitudes below 8 km
1997 WVIOP	15 Sep–6 Oct 1997	Primary results: excellent agreement between chilled mirror and Vaisala capacitive element sensors; excellent agreement in sensitivity (slope of 0.996) in PWV demonstrated between scanning Raman lidar data calibrated to a chilled mirror on the tower and MWR observations; 4%–8% differences still remain in different methods (MWR, sonde, GPS, in situ scaled Raman lidar) to determine PWV; reconfirmed that differences were less than 5% between the two Raman lidars for all altitudes below 8 km; 3%–8% differences between PWV retrieved from the various solar radiometers when using the same model and spectroscopy
1999 Lidar IOP	27 Sep–19 Oct 1999	Primary results: MWR-calibrated Raman lidar was approximately 7% moister than MPI-DIAL during nighttime and was 1%–5% drier during daytime, which is believed to be an artifact of how the Raman lidar was calibrated in the daytime
2000 WVIOP	18 Sep–8 Oct 2000	Goal is to resolve absolute calibration of water vapor:* implementing lessons learned regarding MWR calibration using the tip-curve calibration procedure; use of liquid-nitrogen blackbody targets to validate the calibration of the MWRs during the experiment; MPI-DIAL provides absolute profiling reference; scanning Raman lidar calibrated to well-characterized in situ observations on tower (capacitive sensors and chilled mirrors) to compare against other observations of PWV
AFWEX	27 Nov–15 Dec 2000	Goal is to characterize water vapor measurements in upper troposphere:* in situ reference sensors (chilled mirror/frostpoint hygrometer and a tunable laser diode hygrometer) on NASA DC-8 providing ground truth; NASA LaRC LASE DIAL provides absolutely calibrated profiles above and below the DC-8; MPI-DIAL provides absolute profiling reference; scanning HIS and NAST-I (airborne high-spectral resolution infrared radiometers) providing direct observations of effect of atmospheric water vapor on infrared emission

*Analysis is ongoing and is the subject of future papers.

comparison of Radiation Codes in Climate Models (ICRCCM), was initiated because of the central role of radiative processes in climate change. Initially, this program focused on comparing clear-sky longwave radiation calculations (Ellingson et al. 1991). However, due to a lack of high-spectral resolution radiation measurements together with coincident atmospheric state data to drive the models, ICRCCM was unable to evaluate the absolute accuracy of these models. ICRCCM thus recommended that a dedicated field program measure spectral radiance at high resolution simultaneously with the atmospheric state data required to drive these radiation models (Ellingson et al. 1991; Ellingson and Wiscombe 1996). ARM was designed in part to address this need, and thus early activity in the ARM program concentrated on validating a detailed and physically based line-by-line radiative transfer model using atmospheric state data together with high-resolution infrared emission spectra observed at the SGP CART site.

The primary incentive for focusing on water vapor came from the ARM Instantaneous Radiative Flux (IRF) working group. This group was modeling the downwelling longwave radiation at the surface using two tools developed in ARM: 1) the Line-by-Line Radiative Transfer Model (LBLRTM; Clough et al. 1992; Clough and Iacono 1995) and 2) high-resolution downwelling spectra observed by the Atmospheric Emitted Radiance Interferometer (AERI; Revercomb et al. 1993; Feltz et al. 1998). The atmospheric state profiles used to drive the LBLRTM were measured by radiosondes over nearly 4 yr, and the model calculations were compared to the AERI observations for 745 clear-sky periods. There is good correlation between the residuals in precipitable water vapor observed by the microwave radiometer and radiosonde and the residuals between the AERI and the LBLRTM calculation (Figs. 2b–c). This correlation suggests that uncertainties in the radiosonde profiles are the cause for the large variability in the observed minus calculated infrared radiance residuals.

The large variability in longwave radiance residuals, when the model is driven using radiosonde moisture profiles, proved unacceptable for achieving the accuracy goals for the water vapor continuum model (one component of the LBLRTM). Furthermore, assessment of the strength and width parameters of weak water vapor lines was also precluded due to the level of uncertainty in the water vapor profile. The IRF concluded that this uncertainly limited the ability to model downwelling longwave radiation at the surface. This led to the recommendation that a series of WVIOPs be conducted to characterize the uncertainty and absolute accuracy of the operational ARM measurements and to develop techniques to improve

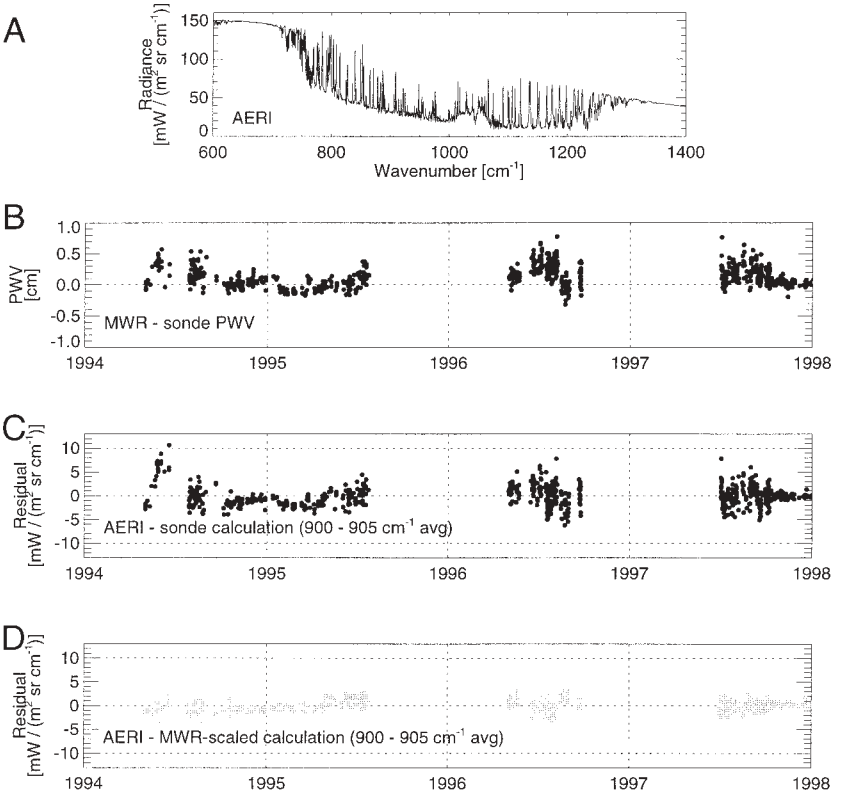

FIG. 2. (a) A typical downwelling infrared radiance spectrum as observed by the AERI. (b) Differences in PWV observed by the ARM MWR and radiosonde. (c) Differences in integrated (from 900 to 905 cm^{-1}) residuals between the AERI observation and the model calculation, where the model was driven by the unscaled radiosonde. The 900–905 cm^{-1} microwindow is transparent (i.e., has few line absorption features) and thus the emission in this window is dominated by the water vapor continuum in clear-sky conditions. For the purposes of computing statistics, these residuals have been detrended to have a mean value of zero. The resulting rms difference is 2.18 mW (m^2 sr cm^{-1})$^{-1}$. (d) Same as in (c) but the model is driven by the MWR-scaled radiosonde, and the rms is 1.11 mW (m^2 sr cm^{-1})$^{-1}$. There are 745 clear-sky cases spread over this 4-yr period.

the water vapor measurements over the site. The IRF wants to constrain the errors in the downwelling flux calculations to less than 1 W m^{-2}, corresponding to an approximate absolute accuracy of 2% in the total column water vapor amount.

The focus of these IOPs is to specify water vapor in the lower troposphere better and thus facilitate the improvement of the downwelling longwave radiance calculations at the surface. With more accurate water vapor measurements, the downwelling radiance calculations and collocated AERI spectra can then be used for their original intent—to improve the absorption models within radiation codes.

The first WVIOP concentrated on characterizing the variability of the moisture profile observed by radiosondes, and in particular in the lowest few kilometers of the troposphere. This experiment demonstrated that significant discrepancies existed among techniques for providing absolute measurements of water vapor. The second WVIOP focused on the absolute accuracy of these measurements.

The ARM program has an unusually powerful array of tools making routine water vapor measurements at the SGP Central Facility (Fig. 1). These instruments include an operational Raman lidar designed specifically for ARM, a dual-channel microwave radiometer, multiple surface-based and tower-based in situ measurements, a two-frequency global positioning system (GPS) antenna, solar and infrared radiometers and spectrometers, and Vaisala radiosondes (see Table 2). For these WVIOPs, additional instrumentation (Table 3) was brought to the site from other institutions to directly address the three hypotheses for the WVIOPs in the lower troposphere. This instrumentation included a scanning Raman lidar, microwave radiometers, chilled-mirror sensors

Table 2. Operational water vapor instrumentation at the ARM SGP Central Facility. (Additional information about the instruments listed may be found online at www.arm.gov/docs/instruments.html.)

Instrument	Primary quantity observed and typical resolutions	References
AERI retrievals	Water vapor mixing ratio profiles: 10 min, 100-m resolution, 24 h day^{-1}	Feltz et al. (1998); Turner et al. (2000)
Cimel sun photometer (CE-318)	Total precipitable water vapor: every quarter air mass for air masses greater than 2, and every 15 min for airmasses less than 2	Holben et al. (1998); Schmid et al. (2001)
GPS at Lamont, OK	Total precipitable water vapor: 30-min resolution, 24 h day^{-1}	Wolfe and Gutman (2000); King and Bock (1996); Rotacher (1992)
In situ probes (Vaisala HMP35D*)	Water vapor mixing ratio: at surface, 25 m, and 60 m; 1-min resolution	Richardson and Tobin (1998); Richardson et al. (2000)
MFRSR	Total precipitable water vapor: 1-min resolution during daytime	Harrison et al. (1994); Schmid et al. (2001)
MWR (Radiometrics WVR-1100)	Total precipitable water vapor: 20-s resolution, 24 h day^{-1}	Liljegren and Lesht (1996); Liljegren (1999)
Radiosonde (Vaisala RS-80H)	Relative humidity profiles: 10-m resolution, eight launches per day	Turner et al. (2003); Lesht (1998)
Raman lidar (CARL)	Water vapor mixing ratio profiles: 10 min, 78-m resolution, 24 h day^{-1}	Goldsmith et al. (1998); Turner and Goldsmith (1999)
RSS	Total precipitable water vapor: 1-min resolution during daytime (installed after the 1996 WVIOP)	Harrison et al. (1999); Schmid et al. (2001)

*Installed after the 1996 WVIOP, replacing the original Qualimetrics 5120-E and 5134-E sensors.

to add redundancy at the in situ locations, a tethersonde and kite system for profiling in the lowest kilometer of the atmosphere, and an additional solar radiometer for retrieval of PWV.

The first hypothesis was that microwave observations of the 22-GHz water vapor line can accurately constrain the total column water vapor amount (i.e., PWV), since the line absorption parameters are well known from the Stark effect laboratory measurements (Clough et al. 1973). If the microwave radiometer (MWR) can be calibrated within 0.5°C, the expected state of the art, then the uncertainty in the retrieved PWV is 0.38 mm. During the 1996 WVIOP, all of the ARM MWRs (eight units) were relocated to the SGP Central Facility for comparison. These instruments measure downwelling microwave radiation at 23.8 and 31.4 GHz. During the 1996 and 1997 WVIOPs (see appendix B for a list of participants in these IOPs), we deployed an independent microwave radiometer from NOAA's Environmental Technology Laboratory (ETL), which measures atmospheric emission at 20.6 and 31.65 GHz. These different systems were used to directly assess the ability to calibrate MWRs and thus test the validity of the hypothesis.

The second hypothesis was that continuous profiling by the Raman lidar provides a stable reference for handling sampling problems and only requires a single height-independent calibration factor. To address this, certain instruments were required to validate the near-field overlap correction of the ARM

Table 3. Additional instrumentation brought to the ARM SGP central facility for the 1996 and1997 WVIOPs.

Instrument	Primary quantity observed and typical resolutions	References
AATS-6	Total precipitable water vapor: 12-s resolution during daytime (during 1997 WVIOP only)	Matsumoto et al. (1987); Schmid et al. (2001)
Chilled mirrors (Meteor AG) on kite and tethersonde	Relative humidity profiles: 2-s data during most evenings	Porch et al. (1998); Turner and Goldsmith (1999)
Chilled mirrors on tower (General Eastern D2/M4)	Dewpoint temperature: 1-min resolution, 24 h day^{-1}[a]	Richardson and Tobin (1998); Richardson et al. (2000)
GPS receiver at SGP Central Facility	Total precipitable water vapor: 30-min data, 24 h day^{-1}	Wolfe and Gutman (2000)
MPI-DIAL	Water vapor density profiles: 30 s, 75-m resolution during multiple 12-h periods (operations restricted by FAA)[b]	Wulfmeyer and Bösenberg (1998); Linné et al. (2001)
NOAA ETL 20.6/31.65-GHz microwave radiometer (ETL 1)	Atmospheric brightness temperatures and total precipitable water vapor:[c] 30-s resolution, 24 h day^{-1}	Hogg et al. (1983); Han and Westwater (2000)
NOAA ETL 23.87/31.65-GHz microwave radiometer (ETL 2)	Atmospheric brightness temperatures and total precipitable water vapor: 30-s resolution, 24 h day^{-1} (during 1997 WVIOP only)	Hogg et al. (1983); Han and Westwater (2000)
Scanning AERI in trailer	Downwelling infrared radiance: 8 min, 1-wavenumber resolution, 24 h day^{-1}	Feltz et al. (1998)
SRL	Water vapor mixing ratio profiles: 1 min, 75-m resolution primarily at night	Whiteman and Melfi (1999); Whiteman et al. (2001)

[a] Chilled mirrors were only deployed on the tower during the 1997 WVIOP only.

[b] The MPI DIAL was only deployed during the 1999 lidar IOP and was the only non-ARM instrument at the SGP site during that experiment.

[c] To convert the brightness temperatures observed from the ETL system to the frequencies used by the ARM systems, the Liebe87 model (Liebe and Layton 1987) was used.

Raman lidar. The ARM Raman lidar requires this correction to account for the mismatch in the alignment of the two channels used to derive the water vapor mixing ratio (Turner and Goldsmith 1999). This mismatch affects data from the surface to approximately 800 m in the low-altitude channels and can be determined directly from data collected by the lidar (Whiteman et al. 1992). The NASA/Goddard Space Flight Center's (GSFC) Raman lidar can scan in a single vertical plane, so we compared far-field data (i.e., data from beyond the range where this correction is required for this system) taken at a small angle above the horizon to the low-altitude data taken by the ARM system. In addition, a tethersonde system and a kite carried a chilled-mirror hygrometer during relatively calm conditions during the 1996 and 1997 WVIOPs. Due to Federal Aviation Administration (FAA) restrictions, these tethered systems remained in the lowest kilometer of the atmosphere.

The third hypothesis was that chilled-mirror hygrometers and capacitive in situ sensors have the accuracy needed to provide a solid, reliable reference at the surface and on the instrumented tower. This was addressed by installing additional moisture sensors at the surface and at 25 and 60 m on the tower. These were capacitive element sensors in 1996 and specially modified chilled-mirror hygrometers in 1997.

As radiosondes are used to measure water vapor in all conditions, the variability of these instruments must be characterized. To this end, more than 100 dual-sonde launches were made during the 1996 and 1997 WVIOPs, where two sonde sensor packages from the same manufacturer flew simultaneously on the same balloon. This allowed us to analyze the differences between two sonde packages with the least uncertainty.

These experiments also compared the absolute calibration of different methods to measure PWV. We integrated radiosonde moisture profiles to directly measure PWV and used brightness temperature observations from the MWR to physically retrieve PWV by inverting accurate radiative transfer models. Another approach coupled the use of accurate in situ sensors and the Raman lidar. By scanning with the NASA Raman lidar to achieve accurate low-altitude observations with good signal-to-noise ratio, the calibration of the in situ sensors in the 60-m tower was transferred to the lidar. Thus, the PWV observations derived from integrating these profiles are calibrated using the in situ sensor. We also used GPS systems, which are a relatively inexpensive way to measure PWV in all atmospheric conditions (e.g., Duan et al. 1996), and compared solar techniques, which rely on absorption of solar radiation in one of the water vapor bands.

Both the 1996 and 1997 WVIOPs produced a wide range of atmospheric conditions, with PWV ranging from near 1 to over 5 cm (Fig. 3). In addition, both IOPs had extensive amounts of clear-sky conditions. This reduces the uncertainty associated with clouds in the water vapor retrievals and calculations of longwave radiance at the surface. It should be noted, however, that when comparing observations from different sensors during these experiments that temporal averaging (typically 10–30 min) was used in an attempt to reduce any uncertainty associated with atmospheric structures such as horizontal convective rolls in the boundary layer.

RESULTS. *Radiosonde characterization.* The ARM program, like many other field programs, relies heavily on Vaisala radiosondes to provide the temperature and moisture profiles required for model calculations. Therefore, we needed to understand the apparent variability in the Vaisala RS-80H moisture measurements (Fig. 2). Many researchers have compared radiosonde moisture data to other sensors,

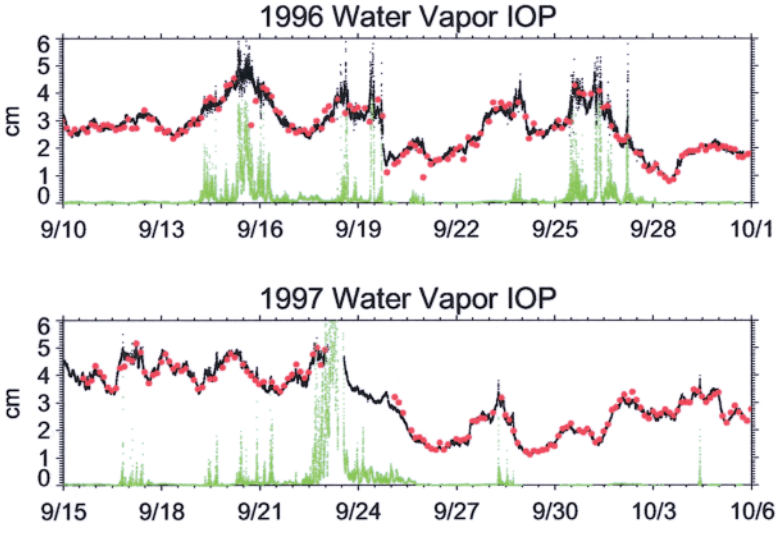

Fig. 3. Time series of PWV (black line) and cloud liquid water (green line) for the 1996 and 1997 WVIOPs as observed by the ETL microwave radiometer. The red circles denote the PWV calculated from radiosonde profiles.

demonstrating that radiosondes appear to have a dry bias (e.g., Guichard et al. 2000; Turner et al. 2000) and underestimate the humidity in the mid- to upper troposphere (e.g., Ferrare et al. 1995). However, one of the obstacles in these comparisons was accounting for temporal and/or spatial differences of the measurements. For example, radiosondes drift away from the launch site and may sample a different air mass than that above the launch site.

The dozens of dual-sonde launches during the WVIOPs provided statistics on how similar instruments from the same manufacturer respond. [Several similar studies have been performed comparing radiosondes from different manufacturers, e.g., Schmidlin (1988).] Two rather startling features were noticed. First, histograms of ratios of PWV from sondes launched together showed peak-to-peak differences of greater than 25%. Second, the differences behaved to first order as an altitude-independent calibration factor in the lower half of the troposphere. Further analysis of the sonde data showed that some of the differences in calibration of the radiosondes appear to depend on the radiosonde "batch," that is, when the radiosonde was manufactured and calibrated (Lesht 1998; Richardson et al. 2000). Figure 4 shows the distribution of the ratio of PWV from 93 dual-sonde launches, of which 40 used radiosondes from different calibration batches. This subset of 40 explains a significant fraction of the spread of the ratio of PWV, but large peak-to-peak differences in the ratio exist where both sondes come from the same calibration batch. An example of a dual launch (Fig. 5) demonstrates the scale-factor nature of the sonde-to-sonde differences.

A 2-yr comparison of PWV observed by the MWR and the radiosondes (launched from the SGP Central Facility) shows large batch-to-batch variability, as the mean PWV ratio (MWR/radiosonde) varies by as much as 15%, with the radiosondes typically being drier than the MWR (Fig. 6). Furthermore, the spread (defined as ±1 standard deviation) within the calibration batch is 8%–12% for most of the batches; the corresponding peak-to-peak differences are then roughly 25% or larger. Note that the variability within the calibration batch is actually larger than the variability between calibration batches.

A correction has been developed by scientists at Vaisala and the National Center for Atmospheric Research Atmospheric Technology Division (NCAR/ATD) (henceforth called the Vaisala correction) to account for the dry bias in Vaisala RS-80 radiosondes due to contamination of the capacitive element sensor (Wang et al. 2002; Guichard et al. 2000; Miller et al. 1999). This correction actually accounts for several humidity measurement errors, including chemical contamination, temperature dependence, basic calibration model, and sensor arm heating (Wang et al. 2002), although for the RS80-H radiosondes that ARM uses, the chemical contamination error dominates the total error. There are two versions of the

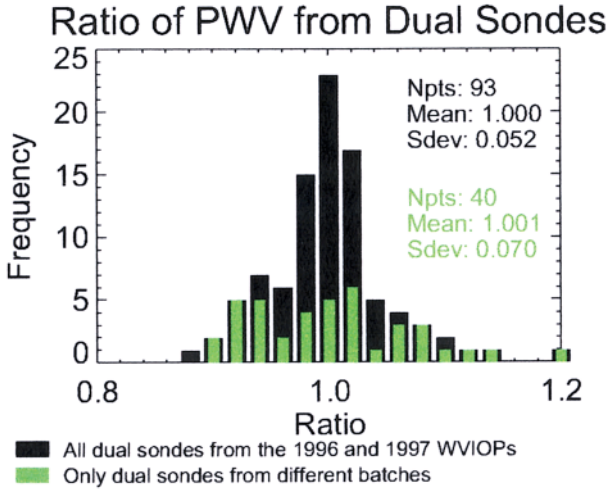

Fig. 4. Distribution of the ratio of PWV derived from each sonde package during the 93 dual launches that were flown during the 1996 and 1997 WVIOPs. The subset of launches that utilized radiosonde packages from different calibration batches is indicated in green.

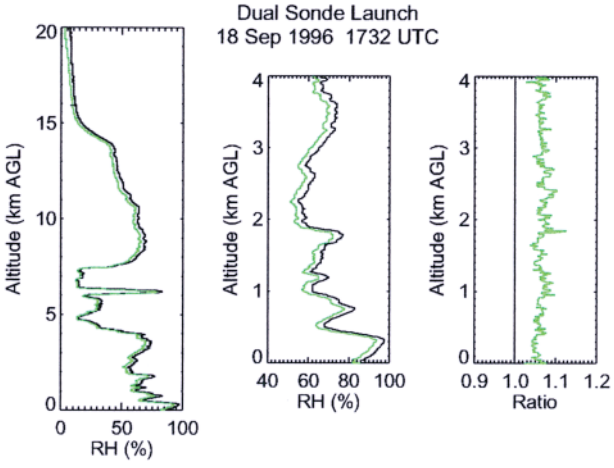

Fig. 5. Typical profiles of relative humidity from the radiosonde packages on a dual-sonde launch during the 1996 WVIOP. Note the height-independent behavior of the ratio of the two in the lower troposphere, where the far right-hand plot shows the ratio of the water vapor mixing ratio derived from each radiosonde package. These radiosondes happen to be from different calibration batches (6231, green, 6322, black), but dual launches that had two radiosondes from the same batch demonstrated the same behavior.

correction, one that utilizes the age of the radiosonde to determine the magnitude of the error that is associated with the chemical contamination, and one that utilizes coincident surface in situ data to estimate this error if the age is unknown. ARM has diligently tracked the serial numbers of the radiosondes it launches from which the age of the radiosonde can be determined, and thus the age-dependent version of the Vaisala correction was used to correct for the dry bias in ARM radiosondes. However, the specified correction appears to only account for the dry bias in a mean sense and does not significantly reduce the overall variability of the radiosondes (Turner et al. 2003).

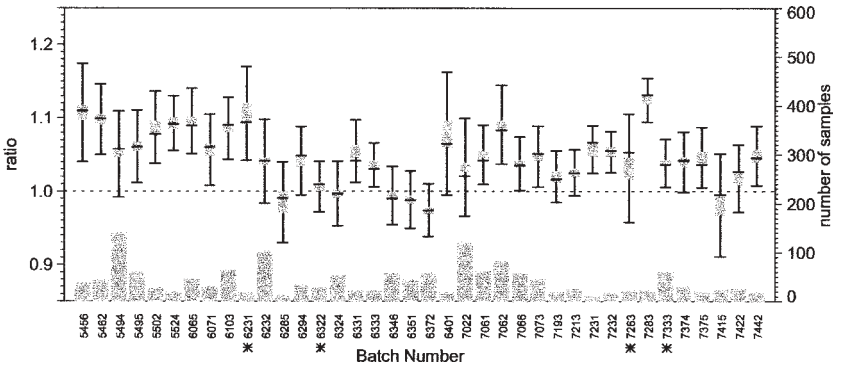

FIG. 6. Analysis of the ratio of the PWV observed by the MWR to the radiosonde as a function of radiosonde calibration batch. The quasi-box-plot indicates the spread (±1 standard deviation about the mean by the error bars and ±1 standard error of the mean by the gray box), the mean value (center of the gray box), and the median ratio (intermediate horizontal black line). The histogram at the bottom indicates the number of radiosondes analyzed in each batch. The standard deviation of the PWV ratio for the 1670 MWR–radiosonde observations, where the mean value for the corresponding batch is removed first, is 0.060. This is almost twice as large as the standard deviation of the mean batch values (0.038 for the 38 batches). Radiosondes launched during the 1996 WVIOP were from batches 6231 and 6322, while radiosondes launched during the 1997 WVIOP were from batches 7263 and 7333. These batches are indicated by the asterisks in the plot.

The MWR data are stable and consistent over time, as compared to the AERI, and thus the radiosonde moisture profile could be scaled to agree with the MWR using a height-independent scale factor as suggested by the dual-sounding results. ARM therefore scales the radiosonde profile to agree with the MWR in terms of PWV; an automated algorithm was developed to do this. This correction significantly reduces the variability of the radiosonde data in the lower troposphere. Use of the scaled profiles markedly reduces the variability of the longwave residuals between the AERI observations and the LBLRTM calculations. The rms difference between these radiances in the 900–905 cm^{-1} microwindow decreased from 2.2 mW $(m^2\ sr\ cm^{-1})^{-1}$ for the unscaled radiosonde model runs (Fig. 2c) to 1.1 mW $(m^2\ sr\ cm^{-1})^{-1}$ for MWR-scaled (Fig. 2d) results. Clough et al. (1999) and Turner et al. (1998) provide more details on MWR-scaled radiosonde water vapor profiles for longwave radiance calculations at the surface.

In situ comparisons. One simple laboratory and field study compared observations from a chilled-mirror hygrometer and a capacitive element in situ probe (Richardson et al. 2000). While the two instruments have different response times and despite the fact that the chilled-mirror hygrometers were not initially created for long-term (~3 weeks) field use, several important results were found. During the 1996 WVIOP, the in situ Qualimetrics probes on towers were found to be inaccurate, especially during high humidity conditions, and were replaced with Vaisala temperature/humidity probes (Richardson et al. 2000). Also, given that these sensors are relatively inexpensive, redundant Vaisala sensors were placed at both the 25- and 60-m levels of the tower. During the 1997 WVIOP, chilled-mirror hygrometers were installed on the instrumented tower alongside the new capacitive sensors. Excellent agreement (better than 2%) between these two very different observation techniques (Fig. 7 shows the results for the comparison at 60 m) demonstrated that good, well-maintained sensors do provide an absolute measure of water vapor. This confirmed the third IOP hypothesis, that in situ data at the surface could be used as a calibration "rock" by showing that the capacitive sensor agrees well with the chilled-mirror technique. This suggests that the radiosonde variability is not inherently due to the capacitive sensor approach, but rather is due to implementation, the calibration, storage time, or other factors.

Tower-scaled Raman lidar observations. During both the 1996 and 1997 WVIOPs, the ARM MWR proved to be a very stable reference when compared to the AERI, ETL MWR, GPS, and other instruments. This stability makes it a good choice as a calibration transfer standard for Raman lidar and radiosonde mois-

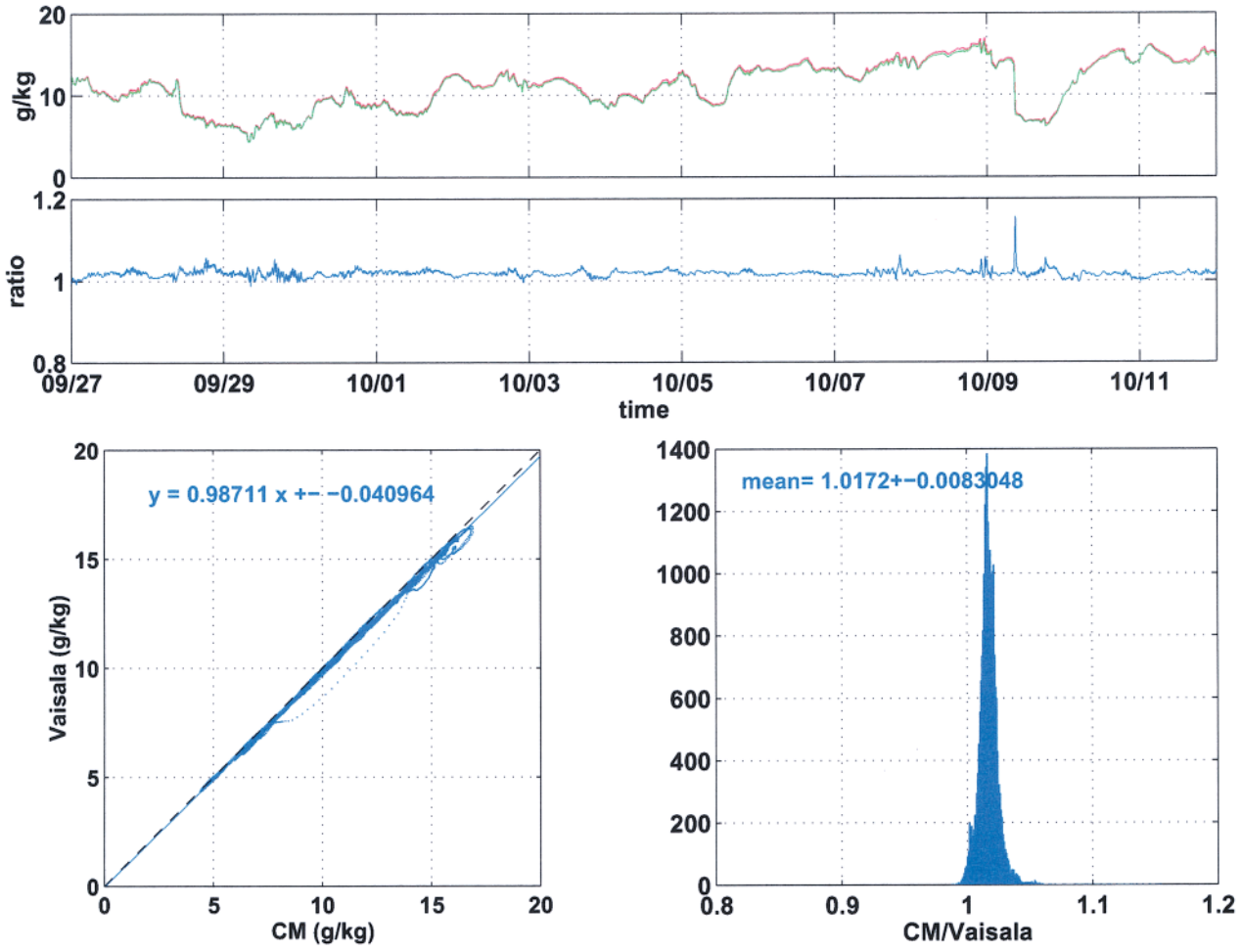

Fig. 7. (top) Time series, (lower left) scatterplot, and (lower right) a histogram of the ratio of the mixing ratio values observed by the Vaisala in situ probes and chilled-mirror hygrometer on the 60-m tower during the 1997 WVIOP.

ture profiles. To gauge the MWR's absolute accuracy, mixing ratio profiles derived from the NASA scanning Raman lidar (SRL) (Whiteman and Melfi 1999; Whiteman et al. 2001) were calibrated using the in situ data from the 60-m tower. The largest zenith angle used by the SRL was 85°, which resulted in an approximate 6.5-m vertical resolution at the 60-m tower. The absolute calibration of the tower in situ observations is transferred into a total column value (assuming a height-independent calibration factor for the Raman lidar) that can then be compared to other total column measurement techniques. The scanning ability of this lidar allows for an improved signal-to-noise ratio at lower altitudes in the boundary layer, as larger slant angles are used to provide data near the surface, and also avoids the use of near-field data from the lidar system. After scaling each SRL profile to agree with mean value observed by the chilled-mirror hygrometer on the 60-m tower during the SRL observation period (when the SRL data were being collected at large zenith angles), the vertical profiles were integrated to provide PWV. These tower-calibrated SRL PWV values were then compared against the ARM MWR. This analysis (Fig. 8) implies that the responses of the MWR and chilled mirror agree. However, this comparison does show a well-defined offset, with the ARM MWR wetter than the tower-scaled SRL by 0.95 mm (which translates into a 1.3°C brightness temperature difference at 23.8 GHz). This bias could be caused by errors in the microwave propagation model, the retrieval of PWV using this model, or in measurement errors by the MWR, and work is on going to identify the source of this bias. While this result does not confirm our first hypothesis (that the MWR can provide an absolute measure of the amount of water vapor in the column), it does provide an independent measurement of the uncertainty in the MWR's observations.

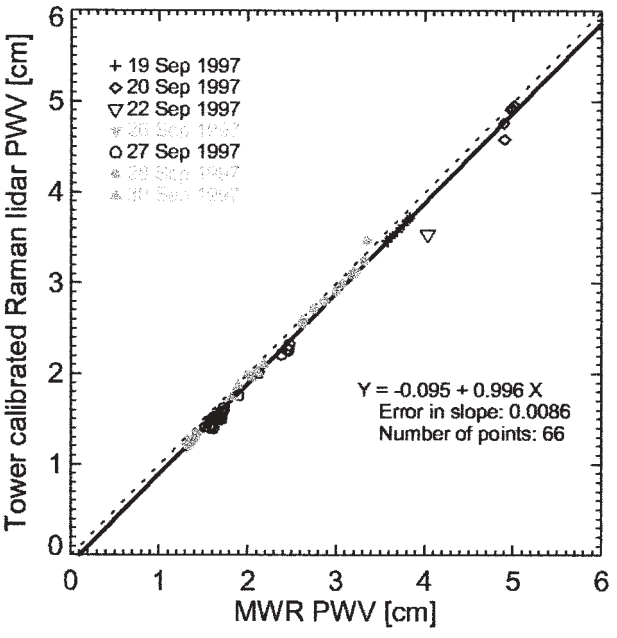

FIG. 8. Comparison of PWV derived from the SRL that was calibrated to agree with the chilled-mirror hygrometer on the 60-m tower with the ARM MWR. The slope (0.996 ±0.009) is very close to unity, indicating that the sensitivity of the MWR agrees with that of the chilled mirror (transferred via the SRL). The slight bias, indicated by the nonzero offset, is not understood.

Raman lidar intercomparison. The second IOP hypothesis—that a Raman lidar only requires a single height-independent calibration within the error of the measurement—would then allow a point or a column-integrated measurement to serve as a calibration transfer standard. Due to the very narrow bandwidth of the interference filters in the CART Raman lidar (CARL) that are used to reduce solar background during daytime operations, there is a slight temperature dependence in the CARL data. However, this is estimated to be less than 2%–3% at 8 km, and thus the assumption of height independence is, to first order, still valid in the lower to midtroposphere.

The hypothesis that the CARL has a height-independent calibration factor is equivalent to stating that the near-field overlap correction derived for the system has been well specified and that there are no unknown system artifacts. Note that this correction is determined directly from calibration data collected by the system (Whiteman et al. 1992; Turner and Goldsmith 1999). To investigate this hypothesis, profiles of water vapor mixing ratio from the SRL were compared with the CARL. The lowest 500 m of the SRL profile were derived from scan data, thus eliminating its overlap correction as a source of error. The comparison of the nighttime mean difference profiles between the two lidar systems, as well as the difference between each lidar system and coincident radiosonde profiles, are given in Fig. 9. For this analysis, both lidars were calibrated to agree with the ARM MWR in PWV. The results from 1996 demonstrate excellent agreement between the two lidars in the lowest 2 km and show a 5% dry bias in the CARL data with respect to the SRL above approximately 3 km. No apparent, significant bias below 8 km is seen between the two lidars during the 1997 WVIOP. Profiles from

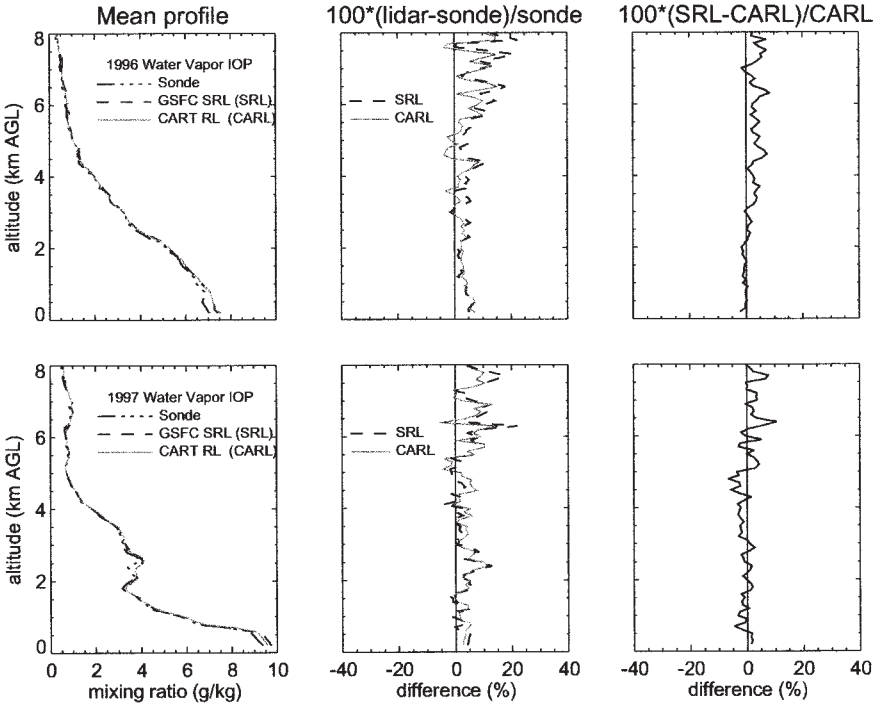

FIG. 9. Comparison of (left) mean profiles from the two Raman lidars and radiosonde, (middle) mean normalized differences between the Raman lidars and the radiosondes, and (right) mean normalized difference between the two Raman lidars during the (upper) 1996 and (lower) 1997 WVIOPs. There are 17 and 11 coincident samples (all nighttime) used in each IOP ensemble, respectively.

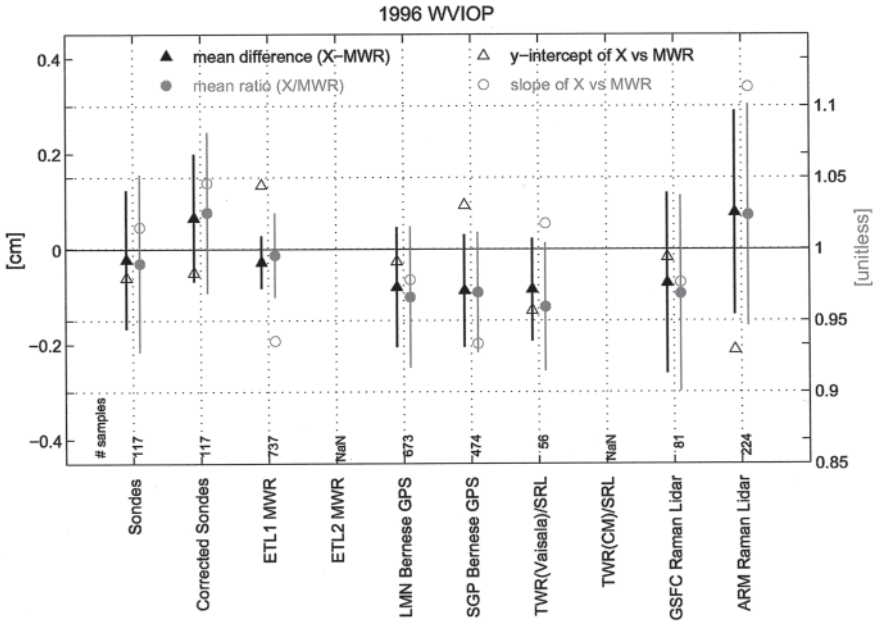

FIG. 10. Comparisons of various techniques that derive PWV with the ARM MWR for the 1996 WVIOP. Data have been averaged to 30-min values before comparison. The mean bias (solid triangles, left axis) and mean ratio (solid circle, right axis), as well as the slope (open circle, right axis) and *y* intercept (open triangle, left axis) of the fitted regression line, are shown. Error bars represent ±1 standard deviation. The number of points used in each intercomparison is indicated along the base of the figure: NaN for the number of samples indicates that no comparisons for this instrument are available, corrected sonde refers to the radiosondes that have been corrected using the Vaisala correction to account for the chemical contamination of the sensor, and TWR(x)/SRL stands for the SRL calibrated to the *x* sensor on the 60-m tower, where *x* is either the chilled mirror (CM) or Vaisala capacitive element probe. The two GPS results are from the station at Lamont, OK (LMN), or the one at the SGP Central Facility (SGP).

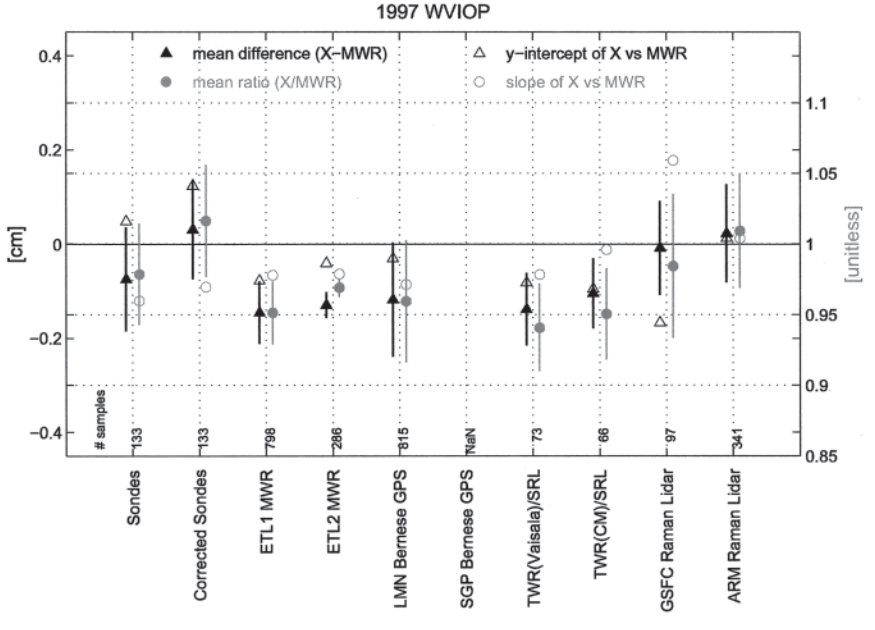

FIG. 11. Same as in Fig. 10 except for the 1997 WVIOP.

both Raman lidars are 4%–10% moister than the radiosonde for both IOPs, which again indicates that the sonde is dry relative to the MWR.

MWR comparisons with radiosondes. Figures 10 and 11 summarize the various techniques for measuring PWV. The spread in the mean data is about 10% among the different techniques for both IOPs. The radiosondes, although variable, are 2%–4% percent drier than the ARM MWR. Applying the Vaisala correction (which accounts for the chemical contamination of the sensor) to the radiosonde data results in the radiosondes being 2%–4% wetter than the ARM MWR during these IOPs. However, Turner et al. (2003), who discuss the characteristics of this correction over a multiyear dataset collected at the ARM SGP site, show that in the long-term mean (i.e., data over multiple years such as in Fig. 6) the corrected radiosondes agree very well with the MWR both in terms of sensitivity and absolute amount. They also demonstrated that the large sonde-to-sonde variability, both within and between calibration batches, is not reduced by this correction, and that the correction introduces a height-dependent artifact in the moisture profile that is most easily seen during well-mixed afternoon soundings. Therefore, the ARM program has, at this time, decided to forego using this correction and instead reduces the variability in the radiosondes by scaling them to agree with the MWR.

Microwave radiometer intercomparisons. The 1996 WVIOP was perhaps the largest ground-based microwave radiometer intercomparison to date. Eight identical MWRs from the ARM program were relocated to the SGP Central Facility, along with the NOAA/ETL 20.6/31.65-GHz system (ETL 1). During this experiment, agreement in PWV among these nine systems was better than 3% (Liljegren et al. 1997). Figure 12 demonstrates the typical agreement between any two of the ARM instruments.

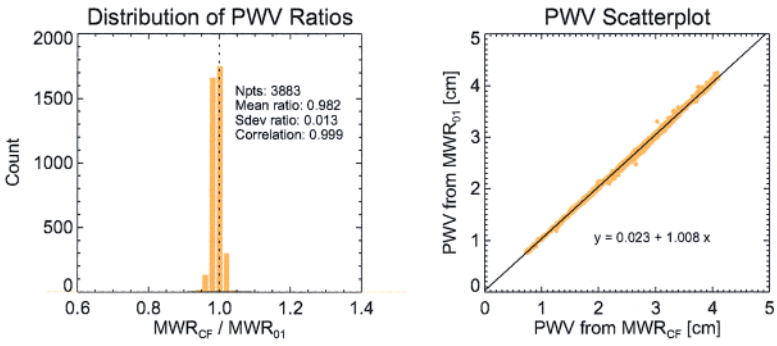

Fig. 12. Comparison of two ARM MWRs (the unit normally deployed at the SGP Central Facility and one other) during the 1996 WVIOP. The data were averaged to 5-min intervals for the comparison.

Comparisons of PWV between the ARM MWR and the NOAA/ETL MWRs are mixed. In 1996, the comparison of PWV with the ETL 1 instrument, which observes downwelling microwave emission from the atmosphere at 20.6 and 31.65 GHz, was excellent in the mean, with less than a 2% bias and relatively little variability. However, there was a substantial difference in sensitivity, as indicated by the nonunity slope of the regression line. In 1997, the mean difference was on the order of 5% and comparisons with a second MWR unit from ETL also showed a 3%–4% difference. However, the ETL data showed a nonlinear response as a function of PWV during the 1997 WVIOP (Westwater et al. 1998), which affects the conclusions that can be drawn from this data. Both the ARM and the ETL microwave radiometers use the Liebe87 model (Liebe and Layton 1987) to retrieve PWV from the observed sky brightness temperatures, thus eliminating one possible source of differences. MWRs are often calibrated by collecting data at different air masses (i.e., by pointing the antenna at different zenith angles) when the sky is assumed to be homogeneous; this process is called tip-curve calibration (Hogg et al. 1983). Investigating the calibration data used by all three MWRs during the 1997 campaign, Han and Westwater (2000) concluded that small inhomogeneities in the atmosphere when these tip-curves are taken could result in calibration differences of this magnitude. New software, based in part upon the Han and Westwater (2000) results, has been developed and is now operational on the ARM MWRs. This software greatly increases the frequency of the tip-curve calibration data, reducing it automatically to maintain the calibration of the ARM MWRs (Liljegren 1999).

While the ARM MWR measurements of PWV were stable and showed agreement in sensitivity with the tower-scaled Raman lidar, the MWRs during the 1997 WVIOP occasionally showed differences in brightness temperature greater than 2 K (1.5 mm). This uncertainty in the calibration undermines the ability to apply and to directly validate the first hypothesis. This issue remains an open question and was addressed again during the 2000 WVIOP.

MWR comparisons with GPS. Total precipitable water vapor can be retrieved from the observed hydrostatic delay measured by ground-based GPS units, which provides a relatively inexpensive way to measure integrated water vapor under a variety of weather conditions (e.g., Duan et al. 1996; Tregoning et al. 1998). GPS data were collected at two locations during the IOPs: by a temporary receiver at the Central Facility and by the NOAA Forecast Systems Laboratory (FSL) at Lamont, Oklahoma (9 mi northwest). Data from both sites were processed using both the GPS at Massachusetts Institute of Technology (GAMIT; King and Bock 1996) and Bernese (Rothacher 1992) software packages. These two analysis packages are very sensitive to input parameters, such as the elevation cutoff angle, and thus we have tried to process data from each IOP identically with each software package. Both techniques use the so-called absolute method (Duan et al. 1996; Wolfe and Gutman 2000) to retrieve PWV, which does not require a reference PWV observation by another instrument. The GAMIT package processed data for 1997 and the Bernese package processed data for both years utilizing a cutoff angle of 7°. The GAMIT processed data for 1996, however, used a cutoff angle of 15°, which resulted in a large dry bias. Even with the same cutoff angle, the GAMIT-processed results were also consistently 3%–4% drier than the Bernese-processed results. Whiteman et al. (2001) also noted this bias between the two algorithms. Recent reanalysis has uncovered a source of error in the GAMIT retrievals used for this analysis, resulting in nearly identical PWV retrievals

from each (S. Gutman 2001, personal communication). The GPS results, represented by the Bernese GPS bullets in Figs. 10 and 11, show that the GPS PWV is about 3%–4% drier than the ARM MWR. A detailed analysis of the GPS data collected at the SGP site is given in Wolfe and Gutman (2000).

MWR comparisons with tower-scaled Raman lidar. As discussed previously, using the NASA SRL as a transfer standard to PWV allows in situ sensors to be compared to the MWR results. While the agreement between the chilled-mirror-calibrated SRL and MWR PWV showed a slope of 0.996, the offset translates into a 3%–4% difference, as shown in Fig. 11. Using the Vaisala probes on the 60-m tower to scale the SRL profiles demonstrates that the sensitivity to water vapor by the capacitive element probe on the tower is within 2% of the sensitivity of the MWR, but that small offsets, which result in small biases, exist.

Calibration stability in the Raman lidars. To gauge the stability of the CART Raman lidar system over time, a single-calibration factor was applied to the entire Raman lidar dataset for each WVIOP. This single-calibration factor was determined from the ARM MWR using a subset of the nighttime data. The CARL profiles of water vapor, calibrated with this single factor for the entire IOP, were then compared to the ARM MWR, with the results shown in Figs. 10 and 11. The positive bias of the CARL results in 1996 is attributed to sunrise–sunset periods, when large solar backgrounds saturated the lidar's photomultiplier tubes before the system switched into its daytime mode (Turner and Goldsmith 1999). Changing the time when the system switches between its daytime and nighttime modes yielded results with little bias between the CARL and MWR during the second IOP. The variability in this intercomparison is dominated by the daytime PWV retrievals from CARL, as the high solar background hampers the ability of the Raman lidar to see high into the troposphere. The standard deviation of the ratio of MWR to CARL PWV is less than 2% at night, as compared to approximately 6% during daytime. Turner and Goldsmith (1999) discuss how PWV is retrieved from the CARL system during the daytime.

Similarly for the NASA SRL, a single-calibration factor was determined and used for each IOP. The SRL results shown in Figs. 10 and 11 are from nighttime data only, as only a small amount of daytime data was collected. The detection optics of the SRL were exposed to the ambient environment (due to the arrangement of the trailer that houses the instrument) when the scanning mirror was deployed. This lack of temperature control could contribute to the variability of the SRL PWV results as compared to the ARM MWR. This lidar was recently modified to rectify this situation, allowing the system to scan in a plane while maintaining strict environmental control around the detection optics (Whiteman et al. 2001).

Solar techniques for retrieving PWV. The comparisons of PWV with the solar radiometers CSPHOT, AATS-6, RSS, and MFRSR (see appendix A for the expanded names of these radiometers) have been extensively covered by Schmid et al. (2001) for the 1997 WVIOP. Initial results from this experiment showed that the PWV retrieved from all of these solar radiometers, where different radiative transfer models were used for each instrument, was between 2% and 6% moister than the ARM MWR. Giver et al. (2000) specified corrections to the water vapor line parameters in the 940-nm region—the spectral region sampled by each of the solar radiometers—that impacted the results considerably. Correcting the water vapor line parameters and using the same radiative transfer model for all of the solar radiometers results in the 8%–13% decrease in the retrieved PWV. Therefore, the PWV retrieved from the solar radiometers is now approximately 6%–14% drier than the ARM MWR. Considerable spread (8%, or 2.2 mm) exists between the PWV retrievals from the different radiometers, which is indicative of other-than-model uncertainties involved in the retrieval. Schmid et al. (2001) discuss the retrieval methods used for each instrument and the differences in more detail.

Raman lidar comparisons with DIAL. A separate water vapor experiment during October 1999 at the SGP CART site is particularly relevant to the absolute calibration issue. The water vapor differential absorption lidar (DIAL) of the Max-Planck-Institut für Meteorologie (MPI) in Hamburg, Germany (Wulfmeyer and Bösenberg 1998), was deployed next to the ARM Raman lidar to assess the performance of both, with respect to available range, resolution, and accuracy. The main results from this experiment (Linné et al. 2001) are summarized below.

For the MPI-DIAL, the available range is almost unaffected by background light, so there is little difference between daytime and nighttime performance. The maximum range that can be reached with good reliability is about 6 km, depending on the vertical distribution of water vapor. A ground-based DIAL generally has difficulty retrieving small amounts of water vapor in the mid- or upper troposphere when

a thick layer of high humidity is presented below. For CARL, the range is quite different for daytime and nighttime. During nighttime, CARL can cover the whole troposphere with very good resolution and relative accuracy, but useful water vapor measurements during the day are restricted to approximately 3 km above the surface. This is due in part to the need to heavily attenuate the signal in the water vapor channel, which has the highest background signal due to the solar contribution, in order for the received signal to remain in the detector's linear range. However, new detection electronics, which were tested in the 2000 WVIOP on the SRL, will increase the daytime range of Raman lidar water vapor measurements.

Comparisons of the absolute accuracy of DIAL and CARL were performed, wherein theRaman lidar was calibrated to the ARM MWR. Due to range restrictions from both systems, the integrated water vapor content in the range 1–3 km during the daytime and 1–6 km during the nighttime was compared. Daytime results show some scatter, but on average the MPI-DIAL is 1%–5% wetter than CARL. In contrast, at night the MPI-DIAL is about 7% drier than CARL. Because this change occurs exactly when the CARL switches to nighttime mode, it is obvious that CARL yielded different results for the two modes during this experiment. The Raman lidar calibration logic has been modified to remove this diurnal feature, and MPI-DIAL data from the 2000 WVIOP will be used to validate that this has been addressed correctly.

With the nighttime measurements of CARL being regarded as more accurate, it remains that the MPI-DIAL shows 7% drier values than the MWR-calibrated CARL. DIAL measurements can be considered to be absolutely calibrated, provided that the absorption line parameters used in the evaluation are correct and that the actual transmitted wavelength is known with sufficient accuracy. There is some debate concerning the accuracy of the absorption line parameters, with differences up to 10% for the wavelength used in the DIAL measurement (720-nm region) from different sources. However, the values used in this analysis (Grossmann and Browell 1989) are considered to be the most reliable. During this IOP, there was no continuous control of the transmitted laser wavelength, and therefore a small error cannot be completely excluded. However, there was no indication that the DIAL's laser was not operating correctly during this experiment, and thus the absolute calibration between the DIAL and the MWR (transferred via the Raman lidar) is still uncertain at the 7% level. This was addressed again during the 2000 WVIOP.

SUMMARY AND FUTURE. The 1996 and 1997 water vapor and 1999 lidar IOPs have provided a wealth of data regarding the quality and accuracy of the water vapor instrumentation at the ARM CART site. Perhaps most importantly, significant variability was found to exist in Vaisala RS-80H radiosonde data—both across and within calibration batches. The dual-sonde launches demonstrated that the differences between any two radiosondes act like an altitude-independent scale factor in the lower troposphere and thus a well-characterized reference can be used to reduce this variability. The ARM program has adopted an approach whereby the radiosonde's moisture profile is scaled such that it agrees with the PWV observed by the MWR (although this research suggests that other observations such as GPS could be used to reduce radiosonde variability at other sites). The MWR scaling significantly reduced the sonde-to-sonde variability by approximately a factor of 2 (Turner et al. 2003; Fig. 2d). The appropriateness of this empirical correction is still being investigated, especially in the upper troposphere. In addition, data collected during these IOPs and from the longer-term ARM operational dataset have shown that the Vaisala correction developed by the manufacturer and NCAR/ATD to account for the dry bias does not reduce the sonde-to-sonde variability and introduces other artifacts as discussed in Turner et al. (2003). However, it should be noted that as of 1 May 2001 ARM is using the new RS-90 radiosonde from Vaisala instead of the RS-80H, and work is under way to characterize this new radiosonde sensor package using data from the 2000 WVIOP and AFWEX.

The first two WVIOPs have also succeeded in showing that two of the three original hypotheses have been met: tower-mounted in situ sensors can serve as an absolute reference and the Raman lidar can serve as a stable transfer standard that requires only a single height-independent calibration factor. These results are for the lower to midtroposphere; the accuracy of Raman lidar observations in the upper troposphere will be discussed in a future paper.

We have been unable to validate the hypothesis that the MWR can absolutely constrain the total column amount of water vapor (i.e., PWV) to better than 2%. Detailed investigations into the tip-curve calibration method used to calibrate the MWRs (Han and Westwater 2000) have provided new insight on calibration uncertainties. These methods need to be tested during another IOP. However, the tower-calibrated scanning Raman lidar results have shown that the sensitivity in the ARM MWR is excellent over a wide range of integrated water vapor. Comparisons

of PWV retrieved from the ARM MWR and the scanning Raman lidar calibrated to the chilled mirror on the tower demonstrate differences of approximately 0.95 mm, which translates into an approximate 1.2°C error in brightness temperature at 23.8 GHz.

To address these outstanding issues of absolute calibration, another water vapor IOP was conducted from 18 September to 8 October 2000 (Revercomb 2000; Table 1). To emphasize microwave brightness temperature calibration issues, the ETL MWR, NASA SRL, MPI-DIAL, and AATS-6 were again deployed at the site. The SRL was scanned in an optimal manner to repeat the tower-scaled analysis. The MPI-DIAL was modified such that the performance of its laser could be much better controlled, significantly reducing the uncertainty in the DIAL's absolute calibration. Additionally, a microwave radiometer from the NASA Jet Propulsion Laboratory was brought to the site to provide a third independent microwave measurement. Furthermore, a liquid-nitrogen blackbody was utilized periodically to test the calibration of the MWRs. Finally, chilled-mirror hygrometers were again installed on the tower to ensure that the capacitive in situ probes are indeed providing the accurate reference required. Analysis of this data is on going and the results from this experiment and the impact on the ARM operational measurements will be the topic of a future paper.

This paper has concentrated on the measurement of water vapor in the lower troposphere. Upper-tropospheric humidity is perhaps even more difficult to measure because of the relatively small amounts of water vapor and extremely cold temperatures. Using lessons learned during the first three WVIOPs, AFWEX was designed and conducted from 27 November to 15 December 2000 to characterize upper-tropospheric measurements of water vapor (Revercomb 2000). The goals of this experiment are listed briefly in Table 1; a more detailed discussion and some initial results are presented in Tobin et al. (2002).

The success of these WVIOPs, coupled with the extensive continuous datasets and special observing capabilities of the ARM program for water vapor, have a wide range of potential implications. Contributions are likely to be significant for improvements in the following areas: 1) radiative transfer models, especially the water vapor continuum and regions of weak water vapor lines (the original objective of the IOPs); 2) remote sensing of water vapor from satellite; 3) validation of satellite products; 4) cloud and aerosol formation parameterizations; 5) atmospheric state for dynamical model input; and 6) understanding the energy budget and atmospheric cooling connection with upper-level water vapor. Advancements in these areas not only benefit the ARM program, but the general scientific community as well.

ACKNOWLEDGMENTS. The Office of Biological and Environmental Research of the U.S. Department of Energy funded this research as part of the Atmospheric Radiation Measurement program.

APPENDIX A: ACRONYMS.

AATS-6	Ames Airborne Tracking Sunphotometer (six-channel)
AER	Atmospheric and Environmental Research, Incorporated
AERI	Atmospheric Emitted Radiance Inteferometer
AFWEX	ARM–FIRE Water Vapor Experiment
ANL	Argonne National Laboratory
ARC	Ames Research Center
ARM	Atmospheric Radiation Measurement program
ATD	Atmospheric Technology Division
BAERI	Bay Area Environmental Research Institute
BNL	Brookhaven National Laboratory
CARL	CART Raman lidar
CART	Cloud and Radiation Testbed
CIMMS	Cooperative Institute for Mesoscale Meteorological Studies
CIRES	Cooperative Institute for Research in Environmental Sciences
CM	Chilled mirror
CSPHOT	Cimel sun photometer
CU	University of Colorado
DIAL	Differential absorption lidar
DOE	Department of Energy
ETL	Environmental Technology Laboratory
FAA	Federal Aviation Administration
FIRE	First ISCCP Regional Experiment
FSL	Forecast Systems Laboratory
GAMIT	GPS at Massachusetts Institute of Technology
GPS	Global Positioning System
GSFC	Goddard Space Flight Center
HIS	High-resolution infrared spectrometer
ICRCCM	Intercomparison of Radiation Codes Used in Climate Models
IOP	Intensive observation period
IRF	Instantaneous Radiative Flux (working group within ARM)
ISCCP	International Satellite Cloud Climatology Project

JCET	Joint Center for Earth Systems Technology
LANL	Los Alamos National Laboratory
LaRC	Langley Research Center
LASE	Laser Atmospheric Sensing Experiment (water vapor DIAL instrument)
LBLRTM	Line-by-Line Radiative Transfer Model
MFRSR	Multifilter rotating shadowband radiometer
MPI	Max-Planck-Institut für Meteorologie, Hamburg, Germany
MWR	Microwave radiometer
NASA	National Aeronautics and Space Administration
NAST-I	NPOESS Aircraft Sounder Testbed—Interferometer
NCAR	National Center for Atmospheric Research
NOAA	National Oceanic and Atmospheric Administration
NPOESS	National Polar-orbiting Operational Environmental Satellite System
NSA	North Slope of Alaska
PI	Principal investigator
PNNL	Pacific Northwest National Laboratory
PWV	Precipitable water vapor
Rms	Root-mean-square
RSS	Rotating shadowband spectrometer
SGP	Southern Great Plains
SNL	Sandia National Laboratories
SRL	Scanning Raman lidar
TWP	Tropical western Pacific
UCAR	University Corporation for Atmospheric Research
WVIOP	Water vapor intensive observation period

APPENDIX B: LIST OF PARTICIPANTS DURING THE 1996 AND 1997 WVIOPS.

Name	Affiliation	Main contribution
B. Balsley	CU	Chilled mirror on kite
J. Barnard	PNNL	ARM MFRSR mentor
J. Bösenberg	MPI	MPI-DIAL PI
S. Clough	AER	LBLRTM analysis
D. Cook	ANL	ARM tower in situ mentor
K. Ertel	MPI	MPI-DIAL operation
K. Evans	NASA GSFC JCET	NASA SRL
W. Feltz	University of Wisconsin—Madison	AERI retrievals; forecaster
R. Ferrare	NASA LaRC[a]	NASA SRL
J. Goldsmith	SNL	ARM Raman lidar mentor
S. Gutman	NOAA/FSL	GPS data analysis—GAMIT
R. Halthore	Naval Research Laboratory[b]	Cimel PWV retrievals
Y. Han	NOAA CIRES	ETL MWR data analysis
M. Jensen	CU	Chilled mirror on kite
R. Knuteson	University of Wisconsin—Madison	AERI and LBLRTM analysis
S. Lehmann	MPI	MPI-DIAL operation
B. Lesht	ANL	ARM radiosonde mentor
J. Liljegren	ANL[c]	ARM MWR data analysis
H. Linné	MPI	MPI-DIAL analysis
S. Melfi	NASA GSFC JCET[d]	NASA SRL
J. Michalsky	University at Albany	MFRSR data analysis
V. Morris	PNNL	ARM MWR mentor
R. Peppler	CIMMS/University of Oklahoma	SGP assistant site scientist
W. Porch	LANL	Chilled mirror on the tethersonde
H. Revercomb	University of Wisconsin—Madison	WVIOP chief scientist
S. Richardson	CIMMS/University of Oklahoma	Chilled mirrors on the surface and tower
B. Schmid	NASA ARC–BAERI	AATS-6 PI
D. Slater	PNNL	RSS data analysis
M. Splitt	University of Utah[e]	SGP assistant site scientist; forecaster
D. Tobin	University of Wisconsin—Madison	WVIOP co-coordinator; AERI and in situ analysis

Name	Affiliation	Main contribution
D. Turner	PNNL[f]	WVIOP co-coordinator; ARM infrastructure liaison; ARM Raman lidar analysis
P. van Delst	University of Wisconsin—Madison	AERI analysis
T. van Hove	UCAR	GPS data analysis—Bernese
E. Westwater	NOAA CIRES	ETL MWR; PI
D. Whiteman	NASA GSFC	NASA SRL; PI
B. Whitney	University of Wisconsin—Madison	Radiosonde analysis

[a] Was at NASA/GSFC when these experiments were conducted.
[b] Was at BNL when these experiments were conducted.
[c] Was at DOE/Ames when these experiments were conducted.
[d] Now retired.
[e] Was at CIMMS/University of Oklahoma when these experiments were conducted.
[f] Currently on leave at the University of Wisconsin—Madison.

REFERENCES

Clough, S. A., and M. J. Iacono, 1995: Line-by-line calculations of atmospheric fluxes and cooling rates: Application to carbon dioxide, ozone, methane, nitrous oxide, and the halocarbons. *J. Geophys. Res.,* **100,** 16 519–16 535.

——, Y. Beers, G. P. Klein, and L. S. Rothman, 1973: Dipole moment of water vapor from Stark measurements of H_2O, HDO, and D_2O. *J. Chem. Phys.,* **59,** 2254–2259.

——, M. J. Iacono, and J. L. Moncet, 1992: Line-by-line calculations of atmospheric fluxes and cooling rates: Application to water vapor. *J. Geophys. Res.,* **97,** 15 761–15 785.

——, P. D. Brown, D. D. Turner, T. R. Shippert, J. C. Liljegren, D. C. Tobin, H. E. Revercomb, and R. O. Knuteson, 1999: Effect on the calculated spectral surface radiances dueto MWR scaling of sonde water vapor profiles. *Proc. Ninth Atmospheric Radiation Measurement (ARM) Science Team Meeting,* San Antonio, TX, U.S. Dept. of Energy. [Available online at http://www.arm.gov/docs/documents/technical/conf_9903/clough99.pdf.]

Duan, J., and Coauthors, 1996: GPS meteorology: Direct estimation of the absolute value of precipitable water. *J. Appl. Meteor.,* **35,** 830–838.

Ellingson, R. G., and W. J. Wiscombe, 1996: The Spectral Radiance Experiment (SPECTRE): Project description and sample results. *Bull. Amer. Meteor. Soc.,* **77,** 1967–1985.

——, J. Ellis, and S. Fels, 1991: The intercomparison of radiation codes used in climate models: Long wave results. *J. Geophys. Res.,* **96,** 8929–8953.

Feltz, W. F., W. L. Smith, R. O. Knuteson, H. E. Revercomb, H. M. Woolf, and H. B. Howell, 1998: Meteorological applications of temperature and water vapor retrievals from the ground-based Atmospheric Emitted Radiance Interferometer (AERI). *J. Appl. Meteor.,* **37,** 857–875.

Ferrare, R. A., S. H. Melfi, D. N. Whiteman, K. D. Evans, F. J. Schmidlin, and D. O'C. Starr, 1995: A comparison of water vapor measurement made by Raman lidar and radiosondes. *J. Atmos. Oceanic Technol.,* **12,** 1177–1195.

Giver, L. P., C. Chackerian Jr., and P. Varanasi, 2000: Visible and near-infrared H_2 ^{16}O line intensity corrections for HITRAN-96. *J. Quant. Spectrosc. Radiat. Transfer,* **66,** 101–105.

Goldsmith, J. E. M., F. H. Blair, S. E. Bisson, and D. D. Turner, 1998: Turn-key Raman lidar for profiling atmospheric water vapor, clouds, and aerosols. *Appl. Opt.,* **37,** 4979–4990.

Grossmann, B., and E. V. Browell, 1989: Spectroscopy of water vapor in the 720 nm wavelength region: Line strengths, self-induced pressure broadenings and shifts, and temperature dependence of linewidths and shifts. *J. Mol. Spectrosc.,* **136,** 264–294.

Guichard, F., D. Parsons, and E. Miller, 2000: Thermodynamic and radiative impact of the correction of sounding humidity bias in the Tropics. *J. Climate,* **13,** 3615–3624.

Han, Y., and E. R. Westwater, 2000: Analysis and improvement of tipping calibration for ground-based microwave radiometers. *IEEE Trans. Geosci. Remote Sens.,* **38,** 1260–1276.

Harrison, L., J. Michalsky, and J. Berndt, 1994: Automated multi-filter rotating shadowband radiometer: An instrument for optical depth and radiance measurements. *Appl. Opt.,* **33,** 5188–5125.

——, M. Beauharnois, J. Berndt, P. Kiedron, J. Michalsky, and Q. Min, 1999: The Rotating Shadowband Spectroradiometer (RSS) at SGP. *Geophys. Res. Lett.,* **26,** 1715–1718.

Hogg, D. C., F. O. Guiraud, J. B. Snider, M. T. Decker, and E. R. Westwater, 1983: A steerable dual-channel microwave radiometer for measurement of water vapor and liquid in the troposphere. *J. Climate Appl. Meteor.,* **22,** 789–806.

Holben, B. N., and Coauthors, 1998: AERONET: A federated instrumented network and data archive for aerosol characterization. *Remote Sens. Environ.,* **66,** 1–16.

King, R. W., and Y. Bock, 1996: Documentation of the GAMIT GPS analysis software, version 9.4. Massachusetts Institute of Technology and Scripps Institution of Oceanography, 192 pp.

Lesht, B. M., 1998: Uncertainty in radiosonde measurements of temperature and relative humidity estimated from dual-sonde soundings made during the September 1996 ARM water vapor IOP. Preprints, *10th Symp. on Meteorological Observations and Instrumentation,* Phoenix, AZ, Amer. Meteor. Soc., 80–83.

Liebe, H. J., and D. H. Layton, 1987: Millimeter-wave properties of the atmosphere: Laboratory studies and propagation modelling. NTIA Rep. 87-24, National Telecommunications and Information Administration, Boulder, CO, 74 pp.

Liljegren, J. C., 1999: Automatic self-calibration of ARM microwave radiometers. *Microwave Radiometry and Remote Sensing of the Earth's Surface and Atmosphere,* P. Pampaloni and S. Paloscia, Eds., VSP Press, 433–441. [Available online at http://www.arm.gov/docs/instruments/publications/mwr_calibration.pdf.]

——, and B. M. Lesht, 1996: Measurements of integrated water vapor and cloud liquid water from microwave radiometers at the DOE ARM cloud and radiation testbed in the U.S. Southern Great Plains. *Proc. Int. Geoscience and Remote Sensing Symp. (IGARSS),* Lincoln, NE, U.S. Dept. of Energy, 1675–1677.

——, E. R. Westwater, and Y. Han, 1997: A comparison of integrated water vapor sensors: WVIOP-96. *Proc. Seventh Atmospheric Radiation Measurement (ARM) Science Team Meeting,* San Antonio, TX, U.S. Dept. of Energy. [Available online at http://www.arm.gov/docs/documents/technical/conf_9903/lill-97.pdf.]

Linné, H., D. D. Turner, J. E. M. Goldsmith, T. P. Tooman, J. Bösenberg, K. Ertel, and S. Lehmann, 2001: Intercomparison of DIAL and RAMAN lidar measurements of humidity profiles. *Advances in Laser Remote Sensing: Selected Papers Presented at the 20th International Laser Radar Conference,* D. Dabas, C. Loth, and J. Pelon, Eds., Ecole Polytechnique, 293–298.

Matsumoto, T., P. B. Russell, C. Mina, W. Van Ark, and V. Banta, 1987: Airborne tracking sunphotometer. *J. Atmos. Oceanic Technol.,* **4,** 336–339.

Miller, E. R., J. Wang, and H. L. Cole, 1999: Correction for dry bias in Vaisala radiosonde RH data. *Proc. Ninth Atmospheric Radiation Measurement (ARM) Science Team Meeting,* San Antonio, TX, U.S. Dept. of Energy. [Available online at http://www.arm.gov/docs/documents/technical/conf_9903/miller-er-99.pdf.]

Porch, W., B. Balsley, H. Cole, M. Jensen, B. Lesht, J. Liljegren, S. Richardson, and H. Revercomb, 1998: Application of tethered balloon and kite measurements using chilled mirror hygrometers during the ARM WVIOP in the fall of 1996 in Oklahoma. Preprints, *10th Symp. on Meteorological Observations and Instrumentation,* Phoenix, AZ, Amer. Meteor. Soc., 10–15.

Revercomb, H. E., 2000: Science plan for the 3rd ARM Water Vapor IOP and the ARM–FIRE Water Vapor Experiment (AFWEX) at the ARM SGP CART site, Lamont, OK, U.S. Dept. of Energy, 10 pp. [Available online at http://www.arm.gov/docs/iops/2000/sgp2000afwex/afwex_9.pdf.]

——, F. A. Best, R. G. Dedecker, T. P. Dirkx, R. A. Herbsleb, R. O. Knuteson, J. F. Short, and W. L. Smith, 1993: Atmospheric Emitted Radiance Interferometer (AERI) for ARM. Preprints, *Fourth Symp. on Global Climate Change Studies,* Anaheim, CA, Amer. Meteor. Soc., 46–49.

Richardson, S. J., and D. C. Tobin, 1998: In situ moisture measurements using chilled mirror sensors. *Proc. Eighth Atmospheric Radiation Measurement (ARM) Science Team Meeting,* San Antonio, TX, U.S. Dept. of Energy. [Available online at http://www.arm.gov/docs/documents/technical/conf_9803/richardson-98.pdf.]

——, M. E. Splitt, and B. M. Lesht, 2000: Enhancement of ARM surface meteorological observations during the fall 1996 water vapor intensive observation period. *J. Atmos. Oceanic Technol.,* **17,** 312–322.

Rothacher, M., 1992: Orbits of satellite systems in space geodesy. Ph.D. thesis, University of Bern, Bern, Switzerland, 243 pp.

Schmid, B., and Coauthors, 2001: Comparison of columnar water-vapor measurements from solar transmittance methods. *Appl. Opt.,* **40,** 1886–1896.

Schmidlin, F. J., 1988: WMO international radiosonde intercomparison: Phase II. *Instruments and Observing Methods,* World Meteorological Organization Rep. 29, TD-No. 312, 113 pp.

Stokes, G. M., and S. E. Schwartz, 1994: The Atmospheric Radiation Measurement (ARM) program: Programmatic background and design of the Cloud and Radiation Testbed. *Bull. Amer. Meteor. Soc.,* **75,** 1201–1221.

Tobin, D. C., and Coauthors, 2002: Overview of the ARM/FIRE Water Vapor Experiment. *Proc. 12th Atmospheric Radiation Measurement (ARM) Science Team Meeting,* St. Petersburg, FL, U.S. Dept. of Energy. [Available online at http://www.arm.gov/docs/documents/technical/conf_0204/tobin.pdf.]

Tregoning, P., R. Boers, D. O'Brien, and M. Hendy, 1998: Accuracy of absolute precipitablewater vapor estimates from GPS observations. *J. Geophys. Res.,* **103,** 28 701–28 710.

Turner, D. D., and J. E. M. Goldsmith, 1999: Twenty-four hour Raman lidar water vapor measurements during the Atmospheric Radiation Measurement program's 1996 and 1997 water vapor intensive observation periods. *J. Atmos. Oceanic Technol.,* **16,** 1062–1076.

——, T. R. Shippert, P. D. Brown, S. A. Clough, R. O. Knuteson, H. E. Revercomb, and W. L. Smith, 1998: Long-term analyses of observed and line-by-line calculations of longwave surface spectral radiance and the effect of scaling the water vapor profile. *Proc. Eighth Atmospheric Radiation Measurement (ARM) Science Team Meeting,* San Antonio, TX, U.S. Dept. of Energy. [Available online at http://www.arm.gov/docs/documents/technical/conf_9803/turner-98.pdf.]

——, W. F. Feltz, and R. A. Ferrare, 2000: Continuous water vapor profiles from operational ground-based active and passive remote sensors. *Bull. Amer. Meteor. Soc.,* **81,** 1301–1317.

——, B. M. Lesht, S. A. Clough, J. C. Liljegren, H. E. Revercomb, and D. C. Tobin, 2003: Dry bias and variability in Vaisala RS80-H radiosondes: The ARM experience. *J. Atmos. Oceanic Technol.,* **20,** 117–132.

U.S. Department of Energy, 1996: Science plan for the Atmospheric Radiation Measurement (ARM) program. DOE/ER-0670T, Washington, DC, 80 pp. [Available online at http://www.arm.gov/docs/documents/technical/sciplan/sp_contents.html.]

Wang, J., H. L. Cole, D. J. Carlson, E. R. Miller, and K. Beierle, 2002: Corrections of humidity measurement errors from the Vaisala RS80 Radiosonde—Application to TOGA CARE data. *J. Atmos. Oceanic Technol.,* **19,** 981–1002.

Westwater, E. R., Y. Han, S. I. Gutman, and D. E. Wolfe, 1998: Remote sensing of column integrated water vapor by microwave radiometers and GPS during the 1997 water vapor intensive observation period. *Proc. Eighth Atmospheric Radiation Measurement (ARM) Science Team Meeting,* San Antonio, TX, U.S. Dept. of Energy. [Available online at http://www.arm.gov/docs/documents/technical/conf_9803/westwater-98.pdf.]

Whiteman, D. N., and S. H. Melfi, 1999: Cloud liquid water, mean droplet radius, and number density measurements using a Raman lidar. *J. Geophys. Res.,* **104,** 31 411–31 419.

——, ——, and R. A. Ferrare, 1992: Raman lidar system for the measurement of water vapor and aerosols in the Earth's atmosphere. *Appl. Opt.,* **31,** 3068–3082.

——, and Coauthors, 2001: Raman lidar measurements of water vapor and cirrus clouds during the passage of Hurricane Bonnie. *J. Geophys. Res.,* **106,** 5211–5225.

Wolfe, D. E., and S. I. Gutman, 2000: Developing an operational, surface-based, GPS, water vapor observing system for NOAA: Network design and results. *J. Atmos. Oceanic Technol.,* **17,** 426–439.

Wulfmeyer, V., and J. Bösenberg, 1998: Ground-based differential absorption lidar for water vapor profiling: Assessment of accuracy, resolution, and meteorological applications. *Appl. Opt.,* **37,** 3825–3844.